The M·ADP·P_i State Is Required for Helical Order in the Thick Filaments of Skeletal Muscle

S. Xu,* J. Gu,* T. Rhodes,# B. Belknap,# G. Rosenbaum,§ Gerald Offer,*¶ H. White,# and L. C. Yu*

*Laboratory of Physical Biology, National Institute of Arthritis, Musculoskeletal and Skin Diseases, National Institutes of Health, Bethesda, Maryland 20892 USA; #Department of Physiological Sciences, Eastern Virginia Medical School, Norfolk, Virginia 23501 USA; §Argonne National Laboratory, Chicago, Illinois USA; and ¶Department of Clinical Veterinary Sciences, University of Bristol, Bristol, United Kingdom

ABSTRACT The thick filaments of mammalian and avian skeletal muscle fibers are disordered at low temperature, but become increasingly ordered into an helical structure as the temperature is raised. Wray and colleagues (Schlichting, I., and J. Wray. 1986. *J. Muscle Res. Cell Motil.* 7:79; Wray, J., R. S. Goody, and K. Holmes. 1986. *Adv. Exp. Med. Biol*. 226:49–59) interpreted the transition as reflecting a coupling between nucleotide state and global conformation with M·ATP (disordered) being favored at 0°C and M·ADP·P_i (ordered) at 20°C. However, hitherto this has been limited to a qualitative correlation and the biochemical state of the myosin heads required to obtain the helical array has not been unequivocally identified. In the present study we have critically tested whether the helical arrangement of the myosin heads requires the M·ADP·P_i state. X-ray diffraction patterns were recorded from skinned rabbit psoas muscle fiber bundles stretched to non-overlap to avoid complications due to interaction with actin. The effect of temperature on the intensities of the myosin-based layer lines and on the phosphate burst of myosin hydrolyzing ATP in solution were examined under closely matched conditions. The results showed that the fraction of myosin mass in the helix closely followed that of the fraction of myosin in the M·ADP·P_i state. Similar results were found by using a series of nucleoside triphosphates, including CTP and GTP. In addition, fibers treated by N-phenylmaleimide (Barnett, V. A., A. Ehrlich, and M. Schoenberg. 1992. *Biophys. J.* 61:358–367) so that the myosin was exclusively in the M·ATP state revealed no helical order. Diffraction patterns from muscle fibers in nucleotide-free and in ADP-containing solutions did not show helical structure. All these confirmed that in the presence of nucleotides, the M·NDP·P_i state is required for helical order. We also found that the spacing of the third meridional reflection of the thick filament is linked to the helical order. The spacing in the ordered M·NDP·P_i state is 143.4 Å, but in the disordered state, it is 144.2 Å. This may be explained by the different interference functions for the myosin heads and the thick filament backbone.

INTRODUCTION

In relaxed mammalian and avian skeletal muscle, the structure of the thick filament is strikingly dependent on temperature. The thick filament has three strands (Squire, 1972; Maw and Rowe, 1980) of 9_1 right-handed helices with a 429 Å repeat in 143 Å axial intervals (Huxley and Brown, 1967). At or near physiological temperature (>20°C), the myosin heads (cross-bridges) are helically arranged around the backbone shaft of the filament. However, when the temperature is lowered, the helical structure becomes increasingly disordered (Wray, 1987; Wakabayashi et al. 1988; Lowy et al. 1991; Kensler and Woodhead, 1995; Malinchik et al., 1997).

Wray and colleagues (Schlichting and Wray, 1986; Rapp et al., 1991) proposed that hydrolysis of ATP on the myosin heads could promote their ordering on the filament backbone. The ATP hydrolysis mechanism of actomyosin alternates between myosin intermediates that bind to actin strongly (ADP or no nucleotide in the myosin active site) or weakly (ATP or ADP and P_i bound to myosin):

$$\begin{array}{ccccccccc} & & & \overset{\text{slow}}{} & & \overset{\text{fast}}{} & & & \\ \text{AM} + \text{ATP} & \Leftrightarrow & \text{AM·ATP} & \Leftrightarrow & \text{AM·ADP·Pi} & \rightarrow & \text{AM·ADP} & \rightarrow \text{AM} + \text{ADP} + \text{Pi} \\ \Updownarrow & & \Updownarrow & & \Updownarrow & & \Updownarrow & & \Updownarrow \\ & & & \overset{\text{fast}}{} & & \overset{\text{slow}}{} & & & \\ \text{M} + \text{ATP} & \Leftrightarrow & \text{M·ATP} & \Leftrightarrow & \text{M·ADP·Pi} & \rightarrow & \text{M·ADP} & \rightarrow & \text{M} + \text{ADP} + \text{Pi} \end{array} \quad (1)$$

where M is myosin and A is actin. The myosin, when it is not interacting with actin, is either in the pre-hydrolysis state M·ATP or in the post-hydrolysis state M·ADP·P_i, because the rate of product release is slow. Wray proposed that increasing temperature produced greater order in the thick filament by shifting the equilibrium from the M·ATP state toward the hydrolyzed M·ADP·P_i state. This was based on the observation that the order-disorder transition appeared to follow a similar trend in its temperature dependence to that of the M·ATP $\rightleftarrows$ M·ADP·P_i equilibrium in solution (Taylor, 1977). However, a quantitative correlation between the biochemical state and the structure of the thick filament in muscle fibers was not established.

The purpose of the present study was to critically test whether the helical arrangement of cross-bridges did indeed require the M·ADP·P_i state. Our experiments were designed to compare the effects of temperature on the x-ray pattern of relaxed muscle and on the phosphate burst of myosin hydrolyzing ATP under closely matched conditions. We have also taken advantage of the fact that the equilibrium of the hydrolytic step strongly depends on the nucleotide. For

Received for publication 25 March 1999 and in final form 26 July 1999.

Address reprint requests to Dr. Leepo C. Yu, National Institute of Arthritis, Musculoskeletal and Skin Diseases, National Institutes of Health, Bldg. 6, Room 408, Bethesda, MD 20892-2755. Tel.: 301-496-5415; Fax: 301-402-0009; E-mail: lcyu@helix.nih.gov.

0006-3495/99/11/2665/12 $2.00

GTP, the equilibrium lies strongly in favor of M·GTP; for CTP it lies in favor of the M·CDP·P_i state. We have therefore examined how changing the nucleotide affects the x-ray pattern. We have also blocked the hydrolysis step using N-phenylmaleimide, so that diffraction from muscle exclusively in the M·ATP state could be examined. Muscle fibers were stretched beyond filament overlap to avoid complications arising from actomyosin interactions. Our results show that the M·NDP·P_i state is required for helical order. Preliminary results have been presented previously (Xu and Yu, 1998).

METHODS

Muscle preparation and solutions

Stretched muscle fibers

All experiments were performed on chemically skinned bundles of rabbit M psoas major. Only single bundles, fasciculi, ~0.3 mm × 0.6 mm in cross section that were separated by sheaths of perimysium, were used. The bundles, ~30 mm in length, were dissected with great care (see Xu et al., 1997). A single bundle was mounted in a specimen chamber for x-ray diffraction experiments equipped with a motor (Micro Mo Electronics Inc., St. Petersburg, FL; controller by Aerotech, Pittsburgh, PA) for slow, steady stretching. The bundle with initial sarcomere length (SL) = 2.5 μm was stretched to SL = 4.2 μm in the skinning solution at 5°C over 3–4 h for the non-overlap experiments. Some x-ray diffraction patterns were taken at SL = 2.5 μm under relaxed and rigor conditions. The sarcomere length was monitored by laser light diffraction during stretch. Only those stretched bundles giving a sharp laser pattern and without a single broken fiber were used for the experiments in this paper. The integrity of the fibers was always checked under the microscope immediately before the experiments.

There are several advantages in using muscle fibers stretched to non-overlap. First, the study could be focused on the state of myosin alone without complications introduced by actomyosin interactions. In a relaxed muscle, the myosin molecules are in the weak binding states (Brenner et al., 1982, 1984; Eisenberg and Hill, 1985; Chalovich, 1992) and their affinity to actin is reduced by raising temperature (Kraft et al., 1995). Therefore, in the presence of actin (i.e., at overlap sarcomere lengths), several other states (e.g., A·M·ATP) need to be considered in making interpretations of the x-ray data. At non-overlap sarcomere lengths, such complications are minimized. Secondly, it has been shown that in solution the affinity of S1 for nucleoside triphosphates is weakened by the presence of actin (Sleep and Hutton, 1978). In myofibrils the finding was similar: the nucleotide affinity was the same as that for S1 in solution if the myofibrils stretched to non-overlap, but the affinity is weaker in the overlap (Biosca et al., 1988). In skinned rabbit psoas fibers, the affinity of myosin for nucleotides GTP and for AMP-PNP is weakened by as much as several orders of magnitude at high temperatures (Frisbie et al., 1997, 1998). Therefore, in overlap muscle fibers, nucleotide saturation is difficult to achieve at the temperatures used in the present study. However, by applying nucleotides in the millimolar concentration range to non-overlap muscle fibers, the uncertainty concerning nucleotide saturation is avoided.

Solutions

The following solutions were used for the experiments. 1) Relaxing (MgATP) solution contained (in mM): 2 MgATP, 2 $MgCl_2$, 2 EGTA, 5 DTT, 10 imidazole, 10 creatine phosphate, 133 potassium propionate, pH 7.0, ionic strength (μ) = 170 mM. To complete the ATP-backup system, 109 unit/ml creatine kinase (CPK) was added just before the x-ray experiments. 2) Rigor solution contained (in mM): 2.5 EGTA, 2.5 EDTA, 10 imidazole, 5 DTT, 150 potassium propionate, pH 7.0, μ = 170 mM. 3) NTP-free solution contained (in mM): 2 EGTA, 4 $MgCl_2$, 10 imidazole, 50 glucose, 147 potassium propionate, 5 DTT, 2 unit/ml hexokinase, 0.25 Ap5A, pH 7.0, μ = 170 mM. 4) NTP (or NDP) solutions contained (in mM): 2 NTP (CTP, GTP, ATPγS) or 2 ADP added to NTP-free solution with 6 mM lower potassium propionate, pH 7.0, μ = 170 mM. 5) N-Phenylmaleimide (NPM) solution (in mM): 0.1 NPM, 4 EGTA, 1 $MgCl_2$, 4 MgATP, 125 KCl, 10 imidazole. Before applying the rigor solution or NTP-free solution, the bundles were rinsed several times with a "quick rinse" solution containing (in mM): 5 EGTA, 15 EDTA, 20 imidazole, pH = 7.0, μ = 70 mM (Brenner et al., 1986, 1991).

The temperature of the specimen chamber was maintained by two thermal electric devices controlled by a feedback circuit by Cambion (Cambridge, MA). The temperature of the bathing solution in the chamber was maintained at the preset temperatures ±1°C. The temperature ranged between 4 and 25°C. In order to minimize specimen degradation, most of the experiments were carried out at temperatures at ≤20°C.

During the entire course of the experiments, the solution in the chamber was continuously stirred by a syringe pump at the rate of ~0.5 ml/s to minimize any gradient (e.g., temperature gradient) along the length of the bundles. To reduce radiation damage, the specimen chamber was moved up and down continuously for a length of 6 mm at a constant rate of 4 mm/s by a stepping motor (Aerotech, Pittsburgh, PA).

N-Phenylmaleimide (NPM) treatment of fiber bundles

The treatment was carried out according to Barnett et al. (1992) and Xu et al. (1998). After the fiber bundles were stretched, the bundles were reacted with 0.1 mM NPM for 1 h; the reaction was terminated by replacing the NPM-treatment solution with normal relaxing solution containing 5 mM DTT. Occasionally, an x-ray diffraction pattern was first recorded for control purposes before the NPM treatment.

X-ray source, camera, and detector system

Preliminary experiments were performed in the laboratory at the National Institutes of Health using a rotating anode x-ray generator (Elliott GX-6), a double-mirror Franks camera, and an MAR Research imaging plate detector system (MAR Research, Hamburg, Germany; see Xu et al., 1997 for details). All final data described in this paper were collected at the synchrotron radiation source Beamline X9B of the Regional Center for Time-Resolved Synchrotron Spectroscopy at the National Synchrotron Light Source (NSLS), Brookhaven National Laboratory (BNL), Upton, NY. The optics of the beamline consisted of a double crystal monochromator with a sagittally bent second crystal providing horizontal focusing followed by a dynamically bent, flat mirror providing harmonics rejection and vertical focusing. Si-111 crystals were used as monochromators. The monochromatic x-ray beam was point-focused on the detector but collimated to a size of ~0.6 mm horizontal × 0.4 mm vertical at the specimen; the fiber bundle was vertical. The size of the focal spot was 0.43 mm FWHM horizontal and 0.27 mm FWHM vertical. Specimen-to-detector distance was 1500 mm. An MAR Research imaging plate detector with 0.1 mm × 0.1 mm pixel size was used for collecting the x-ray data.

The exposure time for each pattern was 2 min. The maximum accumulated exposure time for each bundle was ≤20 min. In general, after a series of x-ray exposures on the same muscle bundle, x-ray patterns of the solution background at 5 and 20°C were recorded for 2 min. For the background patterns at the end of a series of exposures, the chamber containing the specimen was shifted horizontally by ~1 mm and exposures of 2–4 min were taken.

Data reduction and analysis

The data were displayed and analyzed on Silicon Graphics Indigo workstations (Mountain View, CA) using a program, Profida, originally written by M. Lorenz (Max Planck Institut of Heidelberg, Germany). The program was modified by Dan Gilroy (Laboratory of Physical Biology, NIAMS,

NIH) to suit the size of the current data and wider dynamic range, and uses a different approach for rotating and translating the x-ray pattern (see Xu et al., 1997 for details). The data in the four quadrants were first rotated, folded, and averaged. The program made slices parallel to the meridion and the equator of the diffraction patterns, and summed the intensities within the slices to generate one-dimensional intensity profiles for further analysis. The widths of the slices were chosen to include the entire widths of the layer lines for following the distribution of intensity along layer lines. The widths of the slices were adjusted with care so changes in the shape of the layer lines were taken into consideration. In most cases, the diffraction patterns were corrected by subtraction of the background pattern taken at the same temperature.

To directly compare the intensities obtained under different conditions with minimum error, diffraction patterns were always recorded from the same bundle for all the conditions of interest (e.g., the temperature change from 5 to 25°C). To quantitatively compare the data from different bundles with different sizes and to input all data for statistical analysis, the integrated intensity of the actin-based 59 Å layer line was used for normalization because of the stability of this reflection in non-overlap fibers. The spacings of all reflections were calibrated at the beginning of this series of experiments by the 1/144.3 $Å^{-1}$ meridional reflection from skinned rabbit psoas muscle in rigor at μ = 170 mM and T = 20°C (see Xu et al., 1997 for details). To correct for contributions from the thin filament and the thick filament backbone to myosin layer lines, in some cases we used difference patterns: normalized patterns obtained in the absence of nucleotide were subtracted from those in the presence of MgATP or MgCTP at the same temperatures (5, 15, and 25°C).

Intensities of the first myosin layer lines from the difference patterns were used to correlate with the biochemical data. Two methods were used to quantify the intensities. 1) Integrated intensities of the first myosin layer line in the difference patterns were obtained with the program PCA (Oxford Instrument, Oakridge, TN); 2) The intensity profiles of the diffraction patterns (in the presence and in the absence of MgATP) were first curve-fitted to subtract the individual background levels, and the difference of the remaining intensities was taken to be the net intensity contributed by myosin cross-bridges. The two methods generally yielded similar results, although the second method is influenced less by individual background levels.

Single turnover measurement of ATP hydrolysis

Chemical quench measurements were made using a computer-controlled stepper motor-driven quench-flow apparatus. Syringes of the quench-flow sample handling unit (Model 27001, Kintek Corp., State College, PA) were driven by a 34A109E stepper motor (Anaheim Automation, Anaheim CA), which was powered by an IMS Panther HI2 microstepper motor controller (Servo-Systems, Montville, NJ). A program written in turbo basic and running on a Zenith 140 PC provided the timing. Solutions of S1 (20 μl) and ATP (15 μl) containing 10,000–20,000 dpm [γ-^{32}P]ATP or GTP (Dupont) were loaded into the sample loops of the 27001 and driven into a delay line by buffer from the drive syringes. After incubation for the desired amount of time, a second drive was used to expel the reaction sample and mix it with acid quench (2 N HCl and 0.35 M KH_2PO_4) to give a final sample volume of 1.0 ml. Mixing times down to 100 ms could be obtained using this pulse configuration. More rapid quench times were obtained using the 27001 in direct drive mode in which the reaction time was varied by changing the flow rate and volume between the mixers. A 0.4-ml portion of the quenched sample was mixed with an equal volume of a 10% slurry of activated charcoal (Sigma, C-4386) in acid quench and centrifuged to remove unhydrolyzed NTP. The total radioactivity of NTP in each sample was determined by directly counting 0.2 ml. The percent hydrolysis was obtained from the ratio of the radioactivity in charcoal treated to directly counted samples after subtracting background from each. Control experiments indicate that >99% of the unhydrolyzed NTP is bound to charcoal. The experiments were done under "single turnover" conditions in which [S1] > [NTP]. The data were then fit to a one- or two-exponential equation using a simplex fitting routine to obtain amplitude and rate information. The rate of the burst is limited by the rate of binding of the ATP to the active site utilizing the relatively low protein concentrations used in these experiments. However, the size of the burst is unchanged as long as $k_{burst} \gg k_s$ (k [steady state]).

RESULTS

Several earlier studies (Wray, 1987; Lowy et al., 1991; Wakabayashi et al., 1988; Xu et al., 1997; Malinchik et al., 1997) showed that rabbit myosin filaments in MgATP-containing relaxing solutions underwent dramatic changes as the temperature is raised from 4 to 25°C. The midpoint of the changes in intensities of the myosin layer lines occurred at ~15°C. In the present study, similar changes (Fig. 1) were found in rabbit psoas muscle fibers stretched to a sarcomere length of 4.2 μm. At 5°C, the myosin-based layer lines are present but weak (Fig. 1 *A*); at 15°C, the myosin

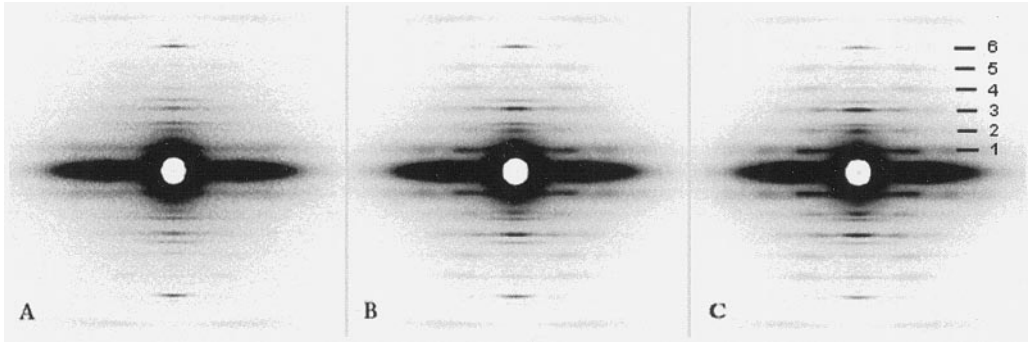

FIGURE 1 X-ray diffraction patterns from a single bundle of skinned rabbit psoas muscle fibers. Sarcomere length (SL) = 4.2 μm. Relaxing solution contained (in mM): 2 MgATP, 2 $MgCl_2$, 2 EGTA, 5 DTT, 10 imidazole, 10 creatine phosphate, 133 potassium propionate, pH 7.0, μ = 170 mM. To complete the ATP-backup system, 109 unit/ml of creatine kinase (CPK) was added just before X-ray experiments. Temperature 5°C (*A*), 15°C (*B*), 25°C (*C*). Patterns were obtained using the synchrotron radiation beamline X9b of National Synchrotron Light Source (NSLS) at Brookhaven National Laboratory (BNL), Upton, NY. Exposure time: 2 min; camera distance: 150 cm. The first- to sixth-order myosin-based layer lines (marked as 1–6 on *C*) can be seen on the patterns, whose intensities clearly increased with temperature. On the meridian the intensity of the third-order reflection (M3) increases with temperature, while the sixth has no significant change with temperature. Note that on the meridian the spacing of the third order is 144.2 Å at 5°C, ~1 Å larger than that at 25°C (143.4 Å).

layer lines are stronger (Fig. 1 *B*); at 25°C, the myosin layer lines are the dominant features of the diffraction pattern (Fig. 1 *C*). The order-disorder transition is therefore intrinsic to the myosin filament and not dependent on interactions with actin.

Single turnover measurements of nucleoside triphosphate

Single turnover measurements of the hydrolysis γ-^{32}P ATP and GTP were measured with a fivefold excess of myosin-S1 to substrate, which provide the most accurate measurement of the ratio of the amplitudes of the rapid pre-steady-state hydrolysis (the phosphate burst) to slower steady-state hydrolysis. The fraction of products complex, M·NDP·P_i, bound to myosin during steady-state hydrolysis was calculated from the ratio of the amplitudes of the slow and fast phases: ffast/(fslow + ffast) = M·NDP·P_i/(M·NTP + M·NDP·P_i). As previously observed under lower ionic strength (Taylor, 1977) the size of the phosphate burst increases from 0.4 at 5°C (Fig. 2 *A*) to >0.9 at 20°C (Fig. 2 *B*). Similar experiments done with GTP (Fig. 2, *C* and *D*) gave much lower bursts and only upper limits of the amplitude of the phosphate burst could be obtained: 0.05 at 5°C and 0.1 at 20°C. The data obtained using GTP fit reasonably well by single exponentials, which are similar to the steady-state rates of GTP hydrolysis. This is in agreement with previous results indicating that the hydrolysis step is rate-limiting for GTP and that M·GTP is the predominant steady-state intermediate from 5 to 20°C (Eccleston and Trentham, 1979; White et al., 1997).

Effects of temperature on the myosin layer lines in the presence of various nucleotides

In ATP

A detailed analysis of the changes in intensities of the myosin-based layer lines in the ATP-containing relaxing solution is shown in Fig. 3. The variation in intensity *along* the first myosin layer line at 5, 15, and 25°C is shown in Fig. 3 *A*. Fig. 3 *B* shows a comparison of intensity *across* the set of layer lines. Both profiles indicate substantial changes in intensities with temperature, but the disorder parameter

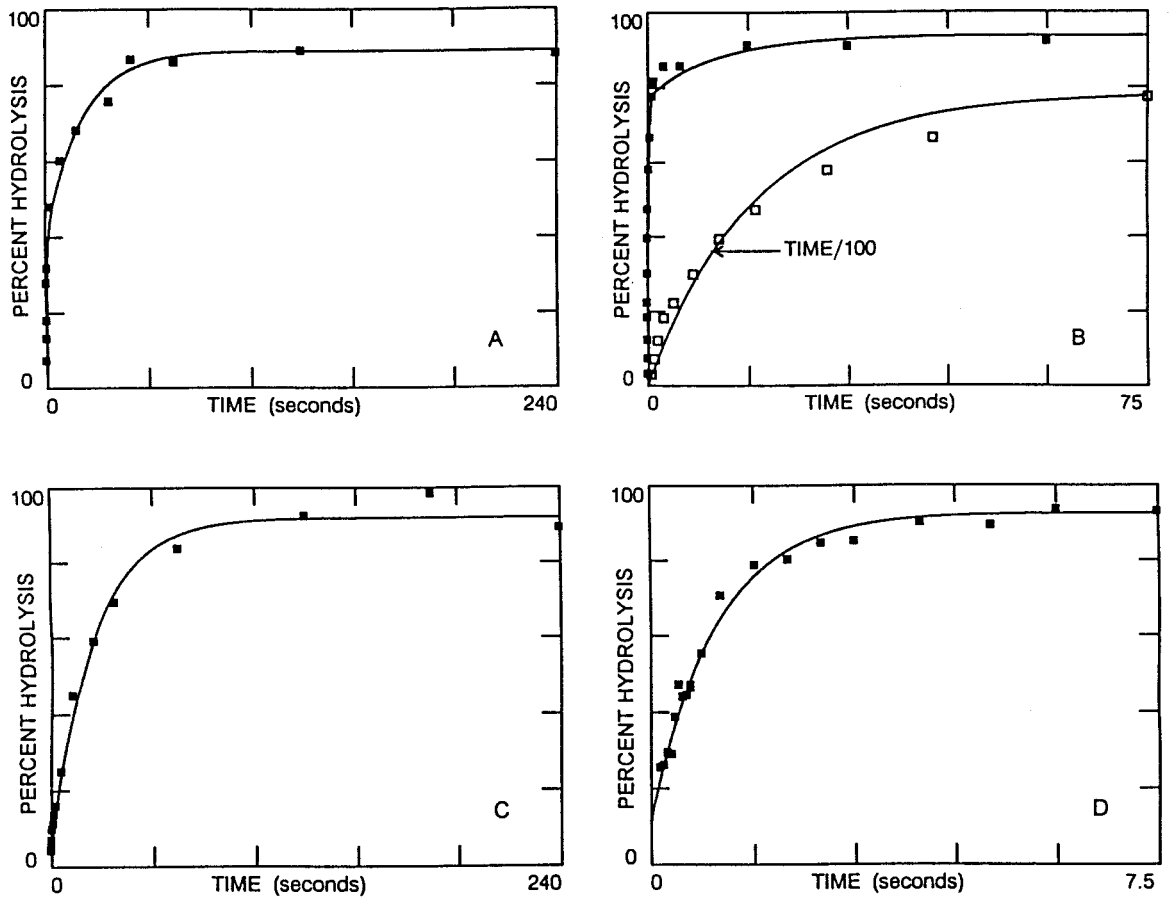

FIGURE 2 Single turnover hydrolysis of MgATP and MgGTP by myosin-S1. A fivefold molar excess of myosin-S1 was mixed with either 1 μM γ-P^{32}-ATP (*A* and *B*) or 5 μM γ-P^{32}-GTP (*C* and *D*) and quenched with acid at the indicated times as described in the Methods. Experimental conditions were (in mM): 147 potassium propionate, 4 $MgCl_2$, 10 imidazole, and 2 EGTA, 0.5 DTT, pH 7 at either 5°C (*A* and *C*) or 25°C (*B* and *D*). The data were fitted by the following curves: (*A*) $F(t) = 0.44\ e^{-1.4t} + 0.56\ e^{-0.03t}$; (*B*) $F(t) = 0.84\ e^{-6.2t} + 0.16\ e^{-0.09t}$; (*C*) $F(t) = 0.94\ e^{-0.04t} + 0.06$; (*D*) $F(t) = 0.89\ e^{-1.0t} + 0.11$.

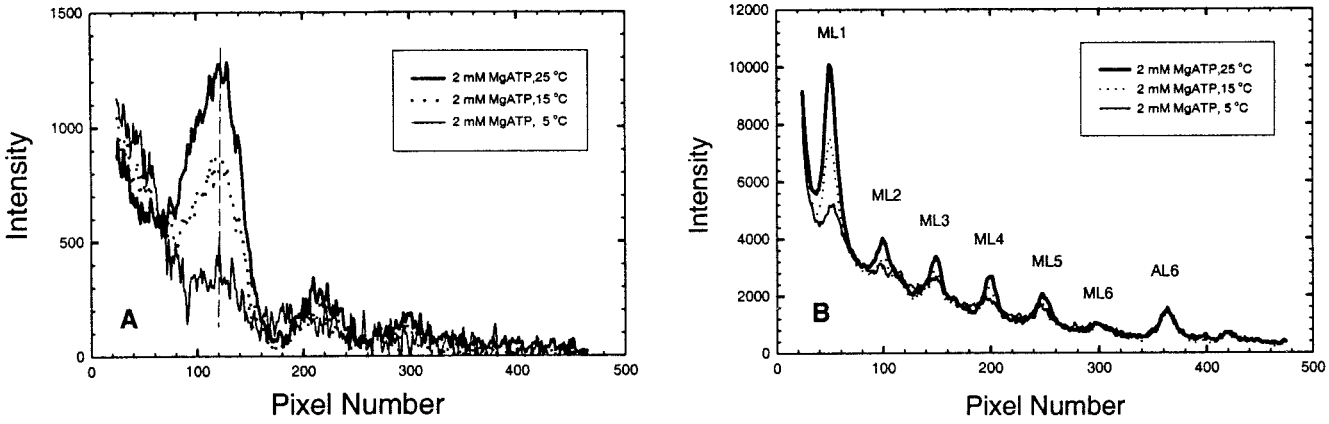

FIGURE 3 Profiles of intensity from the same patterns shown in Fig. 1 at the corresponding temperatures. (*A*) Profiles along the first layer line in Fig. 1. The width of the slice is between 0.00151 $Å^{-1}$ and 0.00286 $Å^{-1}$. The thick solid line was obtained from the pattern in Fig. 1 *C* (25°C); the dotted line was obtained from Fig. 1 *B* (15°C); the thin solid line was obtained from Fig. 1 *A* (5°C). (*B*) Profiles along a line parallel to the meridian. Each slice was centered on the first maximum of the first myosin layer line extending in the direction between 0.00375 $Å^{-1}$ and 0.00733 $Å^{-1}$. The first to the sixth orders of myosin-based layer lines and the sixth and seventh orders of the actin-based layer lines (59 Å and 51 Å) are clearly seen. The net integrated intensity of the first myosin layer line at 5°C decreased to approximately one-fifth of that at 25°C.

(the temperature factor) changes insignificantly because the layer lines maintain approximately the same relative intensities regardless of temperature (Fig. 3 *B*). Moreover, the radial distribution of the intensity of the first myosin layer line remains unchanged with temperature (Fig. 3 *A*). This indicates that the basic structure of the myosin filament is unchanged with lower temperature, but the mass, related to the fraction of myosin heads forming the helical structure, decreases.

In CTP

Several additional nucleotides and analogs with different hydrolysis properties were applied to the stretched fibers. Muscle fibers in the presence of MgCTP shorten and produce force at levels approaching those produced by MgATP (Pate et al., 1993; Regnier and Homsher, 1998). In solution, the equilibrium for CTP hydrolysis is favored more toward the products (M·CDP·P_i) than for ATP (White et al., 1997).

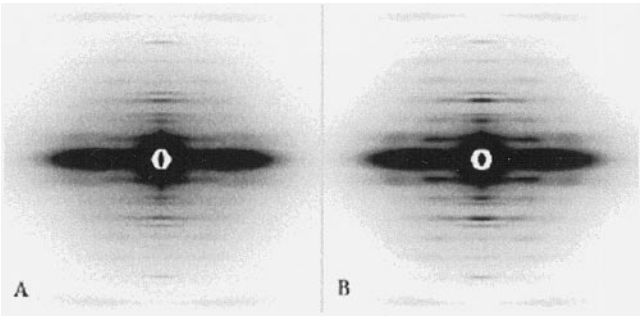

FIGURE 4 X-ray diffraction patterns from a single fiber bundle in relaxing solution containing 2 mM MgCTP. SL = 4.2 μm; μ = 170 mM. (*A*) 5°C; (*B*) 20°C. The first- to sixth-order myosin-based layer lines can be clearly seen even at 5°C. The reflections on the meridian can be indexed to the myosin-based and thin filament-based helical structures, respectively.

Consistent with the solution data, in the stretched muscle fibers in the presence of MgCTP the myosin layer lines are moderately strong even at 5°C (Fig. 4 *A*) and further increase when the temperature is raised to 20°C (Fig. 4 *B*). Profiles across the layer lines (Fig. 5) demonstrate the increase in myosin layer line intensities (after subtraction by those in nucleotide-free solution at the same temperatures) as the temperature was raised from 5 to 20°C (also see Table 1).

In GTP and ATPγS

Diffraction patterns were obtained from stretched fibers in the presence of several other nucleoside triphosphates, GTP and ATPτS, which are not hydrolyzable or slowly hydrolyzable. Intensities from the first myosin layer lines and the equilibrium of nucleotide hydrolysis (M·NTP $\rightleftarrows$ M·NDP·P_i)

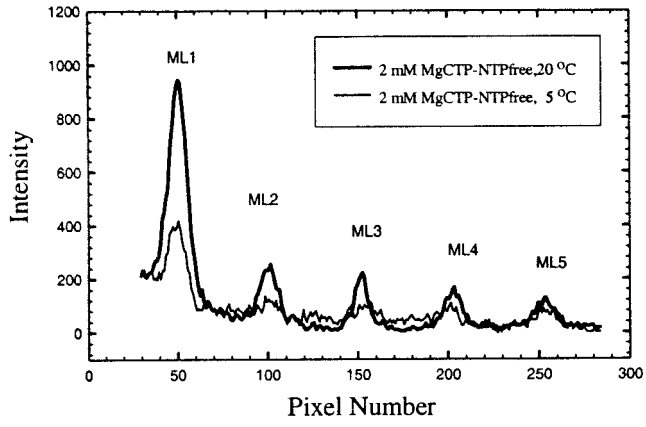

FIGURE 5 Profiles from an axial slice centered at the first maximum of the first myosin-based layer line obtained in 2 mM MgCTP at temperatures as indicated after the pattern is subtracted by the pattern obtained under the nucleotide-free condition.

TABLE 1 Integrated intensities of the first myosin layer lines obtained from the same fiber bundle (except the NPM-treated bundle) in the presence of various nucleotides and analogs

Temperature (°C)	ATP	CTP	GTP	ATPγS	NTP-free	ATP*
5	0.10	0.31	b.d.[#]	b.d.	b.d.	b.d.
20	0.90	1.00	b.d.	b.d.	b.d.	b.d.

All the values of the intensities were normalized to the value obtained in CTP at 20°C.
*From an NPM-treated bundle.
[#]Below detectable level.

by S1 in solution at 5 and 20°C were compared (Table 1). The patterns show very weak myosin layer lines even at 20°C. As explained before, for the GTP equilibrium the fraction of M·GTP stays at >90% for all temperatures studied (<25°C). Similarly, it has been shown that the hydrolytic step is rate-limiting for myosin catalyzed hydrolysis of ATPγS, and the gamma phosphate is even observable in myosin crystals (Gulick et al., 1997). Correspondingly, the myosin layer line intensities were at an undetectable level (<4% of those in the presence of MgATP at 25°C) for GTP and ATPγS.

In nucleotide-free solution

In the diffraction patterns obtained in the absence of nucleotide (NTP-free), features related to a helical distribution of the myosin heads are absent. Besides the well-known features related to the actin filament, there are a few weak but detectable off-meridional layer lines that very likely originate from the troponin on the thin filament and the thick filament backbone. The diffraction patterns are identical at 5°C (Fig. 6 *A*) and at 20°C (Fig. 6 *B*) within experimental error. Details of the analysis will appear elsewhere.

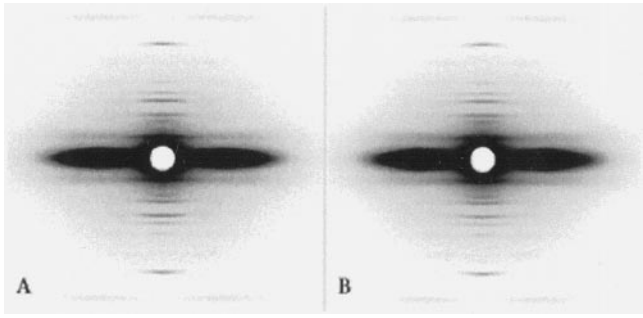

FIGURE 6 X-ray diffraction patterns from a single bundle of skinned rabbit psoas muscle fibers in the absence of nucleotide. SL = 4.2 μm; μ = 170 mM. (*A*) *T* = 5°C; (*B*) 20°C. Myosin-based layer lines are absent, while the related meridional reflections remain rather strong. The spacing of the third meridional reflection is 144.2 Å. The visible layer line in the diffraction pattern most likely originates from the thin filament: the spacing of the first layer line is 380 Å in the inner part close to the meridian; at the outer radius, the spacing is shifted to 365 Å. As the temperature is raised from 5 to 20°C, the diffraction patterns are almost identical. Patterns such as shown here were used as background subtraction from those in nucleotide-containing solutions (see Methods).

In ADP

To determine whether myosin heads with bound MgADP could be arranged in a helical array, diffraction patterns from stretched fibers in the presence of 2 mM MgADP were recorded at 5 and 20°C. The diffraction patterns are hardly distinguishable from those recorded from nucleotide-free solution: in particular, there are no detectable myosin layer lines regardless of temperature. Fig. 7 shows the intensity distributions in the axial direction, revealing features almost identical to those obtained under nucleotide-free conditions.

After inhibition of ATP hydrolysis

To investigate the structures of the M·ATP state alone, the fibers were reacted with NPM, which inhibits the hydrolysis step. The diffraction patterns are almost identical to those obtained in nucleotide-free solution regardless of temperature. Fig. 8 shows the profiles along a line parallel to the meridian in the diffraction patterns from the NPM-reacted muscle fibers in the presence of MgATP at 5 and 20°C. This suggests that in the M·ATP state the myosin heads are disordered.

Estimated mass distributed in the helical array

Difference patterns between those obtained in the presence and absence of ATP were analyzed. The layer lines in the difference patterns index on the 430 Å repeat and therefore arise from the myosin filament alone. Consequently, the intensities of the layer lines are directly proportional to the square of the myosin (cross-bridge) mass in the helical array scattering coherently. The mass on the myosin helix as a function of the temperature is shown in Fig. 9 *A*. The mass fell to 45% as the temperature was lowered from 25 to 5°C. In Fig. 9 *A*, the mass on the helix was normalized to that at 25°C.

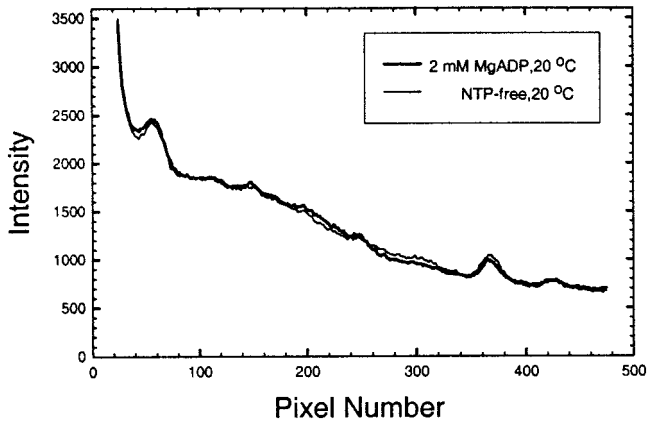

FIGURE 7 Profiles of intensity from axial slices centered at the first maxima of the first myosin layer lines from the patterns under 2 mM MgADP (*thick solid line*) and under NTP-free (*thin line*). There is no significant difference between the profiles obtained at 20°C (shown) and at 5°C (not shown) for both conditions.

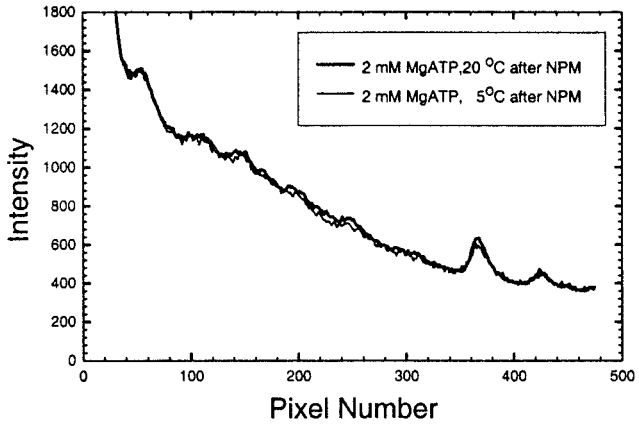

FIGURE 8 Profiles along a line parallel to the meridian at the same radial distance as in Fig. 3 *B* from the x-ray diffraction patterns from a single bundle reacted by NPM. SL = 4.2 μm; μ = 170 mM. In relaxing solution (*thick solid line*) at 5°C; (*thin solid line*) at 20°C. No significant difference can be seen on the profiles.

By analyzing the x-ray diffraction patterns from rabbit psoas muscle at several temperatures, Xu et al. (1997) and Malinchik et al. (1997) suggested that the increase in the myosin-based layer line intensities with increasing temperature was the result of redistribution of the myosin population among three structural states in equilibrium: 1) weakly attached to actin with a random orientation of attachment; 2) detached and disordered; and 3) detached and ordered on the thick filament backbone. In the present study, only structural states 2) and 3) are present. With quantitative data available at several temperatures, the order/disorder equilibrium can now be studied in more detail. The equilibrium constant K_{ord} is defined as

$$K_{ord} = \frac{a}{1-a}$$

where a is the ordered fraction.

The dependence of the equilibrium constant on temperature can be expressed by the Arrhenius relation:

$$\frac{\partial \ln K_{ord}}{\partial 1/T} = -\frac{\Delta H^o}{R}$$

where T is the absolute temperature, ΔH^o is the enthalpy of the transition, and R is the gas constant.

The measured intensities as a function of temperature are only relative to those obtained at one particular temperature, say, at 25°C. The value of a (a_{25}) at that temperature needs to be determined by finding the best fit to the square root of intensities as a function of temperature. The value of a_{25} is less than one, but not by much. Once a_{25} is determined, the value of the maximum amplitude is known, and hence the values of a at all other temperatures can be calculated. We varied the value of a_{25} between the range of 0.5 and 0.99 in the increment of 0.05. For each value of a_{25} a linear regression of log K_{eq} vs. $1/T$ was applied to the data for the best fit of the Arrhenius relation with K_{ord} as a parameter

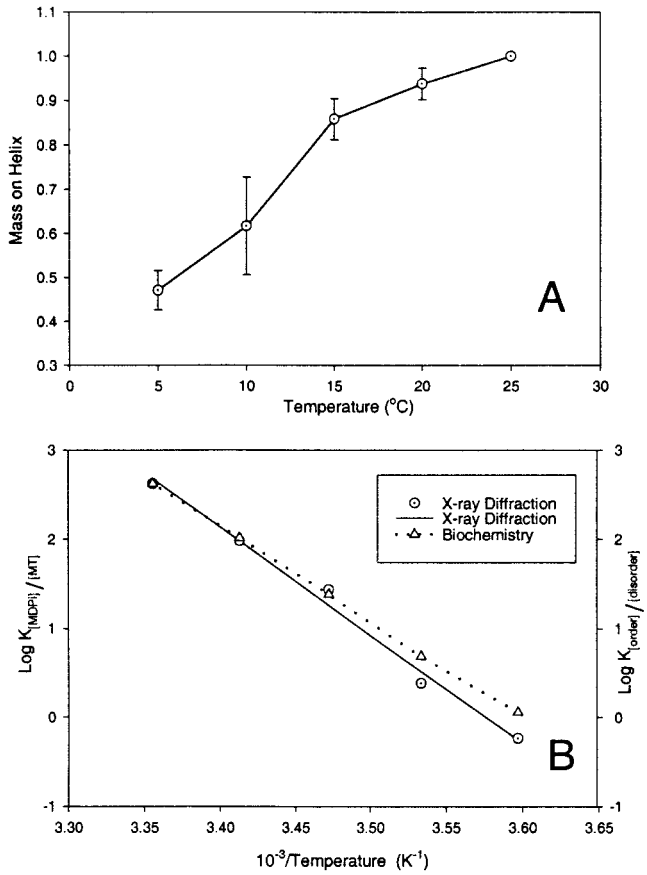

FIGURE 9 (*A*) Changes in coherent (myosin) mass located on the thick filament helix. The mass was calculated as the square root of the integrated intensity of the first myosin layer line. The mass on the helix thus calculated was normalized to that at 25°C. The error bars are standard error of the mean (SEM) with n = 5. (*B*) Arrhenius plot of (ln K_{eq}) vs. $1/T$ (absolute temperature). The K_{eq} for solution data is defined as [M·ADP·P_i]/[M·ATP]; for the helical structure, K_{eq} = [ordered]/[disordered]. The solid line and the dotted line are the best fit to the Arrhenius relation for structure and for biochemistry

$$\ln K_{eq} = -\frac{\Delta H^o}{RT} + \frac{\Delta S^o}{R}$$

For the solution data (*dashed line*), the curve was fitted to four data points at 5, 10, 15, and 20°C. The extrapolated value of K_{eq} at 25°C is 13.8. ΔH^o (solution) = 21 kcal/mole. ΔS^o (solution) = 72 cal/degree·mole. For the coherent mass data, $K_{ord/dis}$ (K [order/disorder]), ΔH^o, and ΔS^o were varied as parameters. The curve-fitting yielded $K_{ord/dis}$ at 25°C = 14, and ΔH^o (order/disorder) = 23 kcal/mole. ΔS^o (order/disorder) = 86 cal/degree·mole.

(MLAB, Civilized Software, Bethesda, MD). The best fit (correlation coefficient = 0.9899) was found with a_{25} = 0.93 and K_{ord} = 15.7 at 25°C (Fig. 9 *B*). The slope yielded the value of ΔH^o = 23.6 kcal/mole. For comparison, ln $K_{hydrolysis}$ (henceforth designated K_{hyd}) vs. $1/T$ is also plotted in Fig. 9 *B*. The values of K_{hyd} over the range of temperature studied and the slope ΔH^o_{hyd} (21.3 kcal/mole) are very similar to those determined for the order/disorder distribution. Thus the structural data further support the idea of ordered/disordered populations being in equilibrium, and strongly coupled to the M·ADP·P_i/M·ATP equilibrium.

The definition for K_{ord} used above assumes that the myosin heads behave independently. Another possibility is that there is cooperativity among the myosin heads to form the ordered array, i.e., it requires dimer pairs of myosin heads both to be in the M·ADP·P_i state to be ordered in the helix (see Note 1 at end of text). In this case the ordered fraction a would be $K_{hyd}^2/(1 + K_{hyd})^2$. Hence $K_{ord} = a/(1 - a) = K_{hyd}^2/(1 + 2K_{hyd})$ or $= K_{hyd}/2$ for $K_{hyd} \gg 0.5$. At low temperature, K_{ord} is indeed less than K_{hyd} by ~0.3, but at 15, 20, and 25°C K_{ord} and K_{hyd} are very similar. The data fit the non-cooperative model more closely, but one cannot rule out such cooperativity.

In estimating the coherent mass in the thick filament helix, an error may originate from the background subtraction method used in the present study (see Methods). The assumption is that the myosin heads do not contribute to the first myosin layer lines obtained under nucleotide-free condition. This could lead to an over-subtraction if weak myosin layer lines were present in the diffraction pattern from the nucleotide-free fibers. However, such an error is believed to be insignificant, because the first myosin layer line, normally the strongest in the diffraction patterns, was below the experimentally detectable level.

Other features of the difference patterns between those in the presence and those in the absence of nucleotides

Spacings of the third-order meridional reflection

There has been a great deal of interest in the dynamic transition of the spacing 143 Å ⇄ 144 Å of the third-order meridional reflection (d_{M3}) when the relaxed muscle enters the rigor state or the contracting state, but its cause has been unclear (Haselgrove, 1975; Huxley, 1979; Irving et al., 1992). Our findings using the stretched muscle fibers are the following (Table 2): 1) In the absence of nucleotide, the spacing of the third-order meridional reflection is 144.2 Å, and remains almost the same at all temperatures studied; 2) In the NPM-reacted fibers (M·ATP only) and in ADP, d_{M3} = 144.2 Å at all temperatures studied, the same as the value in the absence of nucleotide; 3) In the presence of MgATP and MgCTP, at >20°C (M·ADP·P_i; M·CDP·P_i), d_{M3} = 143.4 Å; at low temperatures (5°C), for MgATP, d_{M3} = 144.2 Å; for MgCTP, d_{M3} assumes an intermediate value 143.8 Å. The results suggest that when helical order is present (in the M·NDP·P_i state), d_{M3} is 143.4 Å; if filament is disordered, the spacing is 144.2 Å.

TABLE 2 Spacings of the third-order meridional reflection of stretched fibers in solutions containing various nucleotides at 5 and 20°C

Conditions	Sarcomere Length	$d_{M3} \pm$ SEM (n) (Å) 5°C	20°C
MgATP	4.2	144.34 ± 0.22 (5)	143.42 ± 0.10 (6)
MgCTP	4.2	143.78 ± 0.25 (3)	143.32 ± 0.10 (3)
NPM/MgATP	4.2	144.19 ± 0.06 (3)	144.21 ± 0.02 (2)
MgADP	4.2	144.16 ± 0.04 (4)	144.15 ± 0.15 (2)
NTP-free	4.2	144.16 ± 0.05 (5)	144.10 ± 0.01 (4)
Rigor	2.5	144.4	144.30 (standard)

Spacing of the first myosin layer lines

It is well known that the myosin filament in skeletal muscle is a three-stranded 9/1 helix with an axial repeat of 430 Å (Squire, 1981, 1972). However, the measured spacings (422–424 Å) of the dominant first myosin layer lines in the diffraction patterns from various skeletal muscles, including those of frog sartorius (Huxley and Brown, 1967) and rabbit psoas (at >20°C; Xu et al., 1997) differed from 430 Å. The source of complication could be the interaction between actin and myosin or inadequate spatial resolution of the measurements. Consistent with reported measurements, the present study also yielded a spacing that differed from 430 Å at all temperatures studied. However, the difference patterns between those obtained in MgATP at >20°C (M·NDP·P_i) and those in the absence of nucleotides (no myosin layer lines) yielded a layer line spacing of 428 Å, much closer to the theoretical value (430 Å).

Equatorial spacings

The spacing of the equatorial [1, 0] reflection showed little change as a function of temperature in various solutions (Table 3). The spacing was 266 Å and remained the same regardless of the presence or absence of nucleotide.

DISCUSSION

In this work we have established that only those myosin heads in the M·ADP·P_i state are distributed in the helical array by obtaining a quantitative correlation between the phosphate burst and the coherent mass in the helical array of stretched, relaxed muscle fibers with a series of nucleotide substrates. While M·ATP is not the predominant state at physiological temperature, it occurs as a transient intermediate during hydrolysis, and the transition between the two states is likely to be an important part of the cross-bridge cycle in muscle fibers.

Filament structures of myosin·ATP and myosin·ADP·P_i states are observed separately

One of the difficulties in the past in identifying filament structures with individual biochemical states was that one

TABLE 3 Average lattice spacing d_{10} of the Bragg plane [1, 0] in stretched muscle (SL = 4.2 μm) in ATP containing relaxing solution or NTP-free solution

Conditions	5°C	20°C
ATP	265.7	265.2
NTP-free	265.9	266.9

could not observe the myosin·ATP and myosin·ADP·P_i states separately. By using the NPM-reacted muscle fibers (Barnett et al., 1992; Xie et al., 1999), the myosin·ATP state is isolated, because in NPM-reacted fibers the cleavage step is inhibited (Xie et al., 1999). Yet, when interacting with actin, the NPM-reacted myosin is capable of making transformation from the weakly bound state (A·M·ATP) to the strongly bound rigor state (Xu et al., 1998). Although one cannot exclude the possibility that the modification at SH1 and SH2 of the myosin head could prevent the myosin heads from forming a helical array, the chemical modification does not appear to affect its flexibility for structural transformation. Therefore, we conclude that myosin heads with bound ATP are disordered.

Quantitative correlation between biochemical and structural data

Most of the biochemical measurements in solution in the past were carried out at relatively low ionic strength. In the present study, the ionic and temperature conditions used in the solution studies closely matched those used in the fiber diffraction studies. There is a question as to whether the filamentous state of myosin might affect the equilibrium constant of the hydrolysis step. This equilibrium constant of the hydrolysis step has been estimated from the amplitude of the phosphate burst in relaxed myofibrils (Herrman et al., 1993; Ma and Taylor, 1994; White, 1985) and in muscle fibers (Ferenczi, 1986) to be near 1.0 at 25°C. Such experiments must be done under concentrations in which [ATP] $\gg$ [myosin sites] and are therefore experimentally much more demanding than single turnover experiments such as shown in Fig. 2, and require accurate measurement of the number of myosin sites. There is some evidence that the equilibrium constant of the hydrolysis step decreases with temperature in myofibrils (Herrman et al., 1993; Ma and Taylor, 1994), but the errors are larger and a detailed temperature dependence has not been obtained.

Mechanisms by which nucleotides could affect helical order of the thick filament

The coupling between the degree of helical order of the myosin filaments and the nature of the nucleotides at the active site can be rationalized in terms of the known effect of nucleotides on the conformation of the myosin heads. Tryptophan fluorescence (Bagshaw et al., 1974; Johnson and Taylor, 1978; Sleep and Hutton, 1978), low-angle x-ray and neutron scattering (Wakabayashi, 1992; Mendelson et al., 1996), electron paramagnetic resonance (Ostap et al., 1995), and x-ray crystallography (Fisher et al., 1995; Smith and Rayment, 1996; Gulick et al., 1997; Dominguez et al., 1998; Houdusse et al., 1999) indicate that the conformation of myosin depends on the nucleotide bound. Holmes (1998) has grouped the confirmations generally into two groups: "open" (absence of nucleotide, or ATP, its analogs or ADP bound) and "closed" (transitions state to ADP·P_i). Our data indicate that the nucleotide conditions promoting helical order are strikingly similar to those promoting the "closed" form.

In the myosin molecule the heads are flexibly attached to the tail in the absence of bound nucleotide (Mendelson et al., 1973; Elliott and Offer, 1978; Walker et al., 1988) and flexing within the heads between motor and light chain binding domains has also been observed (Burgess et al., 1997). This flexibility apparent in the molecule must be lost or reduced to form an ordered array of myosin heads on the thick filament. Several mechanisms are possible. First, the conformational change induced by hydrolysis may produce a stiffer myosin molecule, either at the interface between the catalytic and light chain domains or at the head-tail junction. This would reduce the thermal motion of the heads to reveal the helical nature of the packing of the myosin molecules in the thick filament. Such an idea is compatible with the recent findings of the three crystal structural states of S1, where the relative positions of the four major subdomains appear to be the most stable for S1 in the transition state (M·ADP·AlF), whereas the conformations of the nucleotide-free and the ADP states contain flexible "joints" between the subdomains (Houdusse et al., 1999). According to the authors, the ADP-containing structure appears to correspond to an ATP state. Our findings of M·ATP, M·ADP, and M states being disordered while only the M·ADP·P_i state is ordered are consistent with the changing flexibility among the subdomains. For example, according to models for the myosin filament such as those of Malinchik et al., (1997) and of Harford et al. (1998), the two heads of the myosin molecule are splayed and not interacting with other myosins. Stiffening of the heads in the M·ADP·P_i state may explain the helical ordering.

Alternatively, the motor domain of each myosin-ADP-P_i head might interact with a fixed feature of the filament such as the backbone or the head-tail junction of a neighboring molecule such as in the model of Offer et al. (manuscript submitted for publication). In such a case, a head could leave the helical array without affecting the ordering of neighboring heads.

A third possibility is that the motor domain of each head might interact with the motor domain of a neighboring molecule, as in the model of Padron et al (1998). In this case, if a head left the helical array, the neighboring head to which it was bound would also become disordered and cooperativity is implied. However, evidence for cooperativity is not clear.

Crowther et al. (1985), Levine and colleagues (1988; Levine, 1993) and Stewart and Kensler (1986) have published reconstructions of the thick filaments from various species. The two heads of the myosin appear to be splayed, but as yet, the resolution of the reconstructions is insufficient for a detailed modeling on the order/disorder transition mechanism.

The role of temperature on myosin conformation

Our results are consistent with the recent temperature jump results in which transitions between two myosin states were found to occur with ATP at rates consistent with those expected for hydrolysis but not with ADP or in the absence of nucleotide (Jahn et al., 1999). However, a more rapid transition in the fluorescence was also seen with ADP and BeF bound to the active site, indicating that the tryptophan fluorescence enhancement associated with a conformational change need not be coupled to hydrolysis. In addition, we have obtained preliminary results on the thick filament structure in the presence of MgADP + Vi, an order/disorder transition occurs that mimics the conversion of M·ATP to M·ADP·P_i. These results suggest that the coupling observed between hydrolysis and the order/disorder transition may occur in the absence of hydrolysis if the ligands bound to the active site produce a conformational equilibrium constant that is near 1 in an experimentally attainable temperature range (Xu et al., 1999a). The mechanism by which an increase in temperature affects both the hydrolysis equilibrium and the conformation of the heads is not known, but plausibly a stronger hydrophobic interaction might be occurring at higher temperature that favors the ordered state.

The dynamic state of the thick filament in the relaxed state: implications for understanding activation

The hydrolysis of ATP produces a myosin·ADP·P_i state that is thought to be ready to generate force when the myosin head interacts with actin. However, the diffraction data indicate that the equilibrium position of the myosin heads with bound ADP and P_i is near the thick filament surface, away from the thin filament (Malinchik et al., 1997). How are the myosin·ADP·P_i heads in a filament able to bind to the thin filament fast enough to account for activation and to the rapid shortening of muscle? The resolution of this apparent difficulty is that the ordered state is in a rapid, dynamic equilibrium with other weak binding states in the ATPase cycle (i.e., M·ATP and A·M·ADP·P_i) based on biochemical, mechanical, and structural evidence. Structural data from x-ray diffraction patterns of relaxed muscle are incompatible with the idea of a static distribution of ordered/disordered myosin heads (Malinchik et al., 1997; Gu and Yu, submitted for publication). The rate constants for the hydrolysis reaction M·ATP $\rightleftarrows$ M·ADP·P_i are fast (Taylor, 1977). Mechanical stiffness measurement of relaxed muscle also indicated rapid equilibrium between the weak binding states (Brenner et al., 1982). Electron paramagnetic resonance of spin-labeled myosin in isolated filament (Barnett and Thomas, 1987) and in muscle fibers (Ostap et al., 1995) also indicated the populations of the M·ATP and M·ADP·P_i are in dynamic equilibrium. Therefore, as the muscle is activated and the cross-bridges enter into the strong binding states, a redistribution of populations among the equilibrium states can occur rapidly, providing a mechanism for the myosin heads in the helical array to participate in the force generation process.

Relation to results obtained at full overlap

In our previous study (Xu et al., 1997; Malinchik et al., 1997), we examined the temperature-induced structural changes in the thick filament (Malinchik et al., 1997) at SL = 2.5 μm (close to full overlap). At temperatures $\geq$20°C, the intensity distribution along the first myosin layer line was almost identical between the two results. Therefore, the helical structure of the M·ADP·P_i state is not affected by the presence of actin in the relaxed muscle.

At low temperature, however, we observed a different effect compared to no overlap. In the case of full overlap, the myosin heads moved outward with the center of mass shifted from a radius of 135 Å to a radius of 175 Å (Malinchik et al., 1997). In the present study the center of mass does not change with temperature. Preliminary result suggests that the discrepancy arises because of the formation of a significant fraction of the weakly bound cross-bridges in the A·M·ATP state at low temperature (Xu et al., 1999b). In this weakly bound state, the myosin heads (cross-bridges) appear to be close to the thin filament for attachment and yet maintain the helical symmetry of the thick filament. Further details of the structure of the A·M·ATP state will appear elsewhere.

Significance of the findings on the 143.4–144.2 Å transition

A shift of ~1% in the spacing of the third meridional reflection from 143 to 144 Å upon activation was first observed in frog sartorius muscle (Haselgrove, 1975). Because of its strong intensity, changes in intensity of this reflection have been followed in a number of time-resolved studies (Irving et al., 1992; Kress et al., 1986; Piazzesi et al., 1999) as a way of monitoring the interaction of cross-bridges with actin (e.g., head rotation). In the present study it is shown in Table 2 that the transition in spacing is coupled to the transition of the helical $\rightleftarrows$ non-helical array caused by a transition among the biochemical states, not due to attachment of myosin heads to actin. It is reasonable to suppose, therefore, that the 144.2 Å reflection observed in the disordered state is derived from the backbone of the filament, while the 143.4 Å reflection is primarily derived from the helically ordered myosin heads.

A possible explanation of the shift in spacing rests on the bipolar nature of the thick filament and the interference between the two halves of the filament (Rome et al., 1973; Craig, R.W. (1975). If the myosin heads along the entire length of the thick filament diffract coherently, the Fourier transform of the heads along the entire length of the filament can be considered to be the Fourier transform of the array of ~50 crowns in each half of the filament multiplied by the Fourier transform of two points located at the centers

of the two arrays separated by the bare zone (see Note 2) (a separation of ~8700 Å).

At low temperature the diffraction would instead arise from the thick filament backbone. The coiled-coil tail is ~1620 Å long, i.e., not an integral multiple of 144.2 Å. Hence, the electron density of the backbone projected along the axis would rise and fall in steps (periodicity 144.2 Å) as the number of coiled-coil tails in a cross-section rises or falls by 3 (Squire, 1981). This is likely to be the principal contributor to the third-order meridional reflection produced by the backbone. The distance between the centers of the arrays of tails in the two halves of the thick filament will be smaller than the distance between the arrays by the length of the tail (i.e., ~7080 Å). Hence, the interference function will sample the Fourier transform of the ~50 crown array at different positions, resulting in a different spacing of the meridional reflection.

NOTES

1. Consider, for instance, cooperativity between the two heads of the myosin cross-bridges or the thick filament as being made from dimer units, each one made from the head pointing toward the bare zone of one myosin molecule and one pointing toward the Z-disk of the next or simply among the two heads of one cross-bridge.

2. This is an approximation assuming that the axial projected density of myosin heads is approximately symmetrical so that the two arrays can be considered to be related by a translation rather than by a twofold rotation about an axis normal to the filament axis through the bare zone.

The authors thank Dr. Mark Chance and Mike Sullivan of the Regional Center for Time-Resolved Synchrotron Spectroscopy at the National Synchrotron Light Source (NSLS), Brookhaven National Laboratory for their critical support in using the beamline X9B. We also thank Gary Melvin (Laboratory of Physical Biology, National Institute of Arthritis, Musculoskeletal and Skin Diseases, National Institutes of Health) for designing and fabricating instrumentation used in this series of experiments. We express our appreciation to Dr. Sergey Malinchik for stimulating discussions.

REFERENCES

Bagshaw, C. R., J. F. Eccleston, F. Eckstein, R. S. Goody, and D. Trentham. 1974. The magnesium ion-dependent adenosine triphosphatase of myosin. Two-step processes of adenosine triphosphate association and adenosine diphosphate dissociation. *Biochem. J.* 141: 351–364.

Barnett, V. A., A. Ehrlich, and M. Schoenberg. 1992. Formation of ATP-insensitive weakly-binding crossbridges in single rabbit psoas fibers by treatment with phenylmaleimide or para-phenylenedimaleimide. *Biophys. J.* 61:358–367.

Barnett, V. A., and D. D. Thomas. 1987. Resolution of conformational states of spin-labeled myosin during steady-state ATP hydrolysis. *Biochemistry*. 26:314–323.

Biosca, J. A., L. E. Greene, and E. Eisenberg. 1988. Binding of ADP and 5′-adenylyl imidodiphosphate to rabbit muscle myofibrils. *J. Biol. Chem.* 263:14231–14235.

Brenner, B., M. Schoenberg, J. M. Chalovich, L. E. Greene, and E. Eisenberg. 1982. Evidence for cross-bridge attachment in relaxed muscle at low ionic strength. *Proc. Natl. Acad. Sci. USA.* 79:7288–7291.

Brenner, B., L. C. Yu, and J. M. Chalovich. 1991. Parallel inhibition of active force and relaxed fiber stiffness in skeletal muscle by caldesmon: implications for the pathway to force generation. *Proc. Natl. Acad. Sci. USA.* 88:5739–5743.

Brenner, B., L. C. Yu, L. E. Greene, E. Eisenberg, and M. Schoenberg. 1986. Ca^{2+}-sensitive cross-bridge dissociation in the presence of magnesium pyrophosphate in skinned rabbit psoas fibers. *Biophys. J.* 50: 1101–1108.

Brenner, B., L. C. Yu, and R. J. Podolsky. 1984. X-ray diffraction evidence for cross-bridge formation in relaxed muscle fibers at various ionic strengths. *Biophys. J.* 46:299–306.

Burgess, S. A., M. L. Walker, H. D. White, and J. Trinick. 1997. Flexibility within myosin heads revealed by negative stain and single-particle analysis. *J. Cell. Biol.* 139:675–681.

Chalovich, J. M. 1992. Actin mediated regulation of muscle contraction. *Pharmacol. Ther.* 55:95–148.

Craig, R. 1975. Structural studies on the thick filaments of vertebrate skeletal muscle. Ph.D. Thesis, University of London, Chap. 5.

Crowther, R. A., R. Padron, and R. Craig. 1985. Arrangement of the heads of myosin in relaxed thick filaments from tarantula muscle. *J. Mol. Biol.* 184:429–439.

Dominguez, R., Y. Freyzon, K. M. Trybus, and C. Cohen. 1998. Crystal structure of a vertebrate smooth muscle myosin motor domain and its complex with the essential light chain: visualization of the pre-power stroke state. *Cell*. 94:559–571.

Elliott, A., and G. Offer. 1978. Shape and flexibility of the myosin molecule. *J. Mol. Biol.* 123:505–519.

Eccleston, J. F., and D. R. Trentham. 1979. Magnesium ion dependent rabbit skeletal muscle myosin guanosine and thioguanosine triphosphatase mechanism and a novel guanosine diphosphatase reaction. *Biochemistry*. 18:2896–2904.

Eisenberg, E., and T. L. Hill. 1985. Muscle contraction and free energy transduction in biological systems. *Science (Wash. DC)*. 227:999–1006.

Ferenczi, M. A. 1986. Phosphate burst in permeable muscle fibers of the rabbit. *Biophys. J* 50:471–477.

Fisher, A. J., C. A. Smith, J. Thoden, R. Smith, K. Sutoh, H. M. Holden, and I. Rayment. 1995. Structural studies of myosin: nucleotide complexes: a revised model for the molecular basis of muscle contraction. *Biophys. J.* 68:19S–26S.

Frisbie, S. M., J. M. Chalovich, B. Brenner, and L. C. Yu. 1997. Modulation of cross-bridge affinity for MgGTP by Ca^{2+} in skinned fibers of rabbit psoas muscle. *Biophys. J.* 72:2255–2261.

Frisbie, S. M., S. Xu, J. M. Chalovich, and L. C. Yu. 1998. Characterizations of cross-bridges in the presence of saturating concentrations of MgAMP-PNP in rabbit permeabilized psoas muscle. *Biophys. J.* 74: 3072–3082.

Gulick, A. M., C. B. Bauer, J. B. Thoden, and I. Rayment. 1997. X-ray structures of the MgADP, MgATPγS, and MgAMPPNP complexes of the *Dictyostelium discoideum* myosin motor domain. *Biochemistry*. 36: 11619–11628.

Harford, J., M. Cantino, M. Chew, R. Denny, L. Hudson, P. Luther, R. Mendelson, E. Morris, and J. Squire. 1998. Myosin crossbridge configurations in equilibrium states of vertebrate skeletal muscle. Heads swing axially or turn upside-down between resting and rigor. *Adv. Exp. Med. Biol.* 453:297–308.

Haselgrove, J. C. 1975. X-ray evidence for conformational changes in the myosin filaments of vertebrate striated muscle. *J. Mol. Biol.* 92:113–143.

Herrman, C., J. Sleep, P. Chaussepied, F. Travers, and T. Barman. 1993. A structural and kinetic study on myofibrils prevented from shortening by chemical cross-linking. *Biochemistry*. 32:7255–7263.

Holmes, K. C. 1998. A molecular model for muscle contraction. *Acta Crystallogr. A.* 54:t-97.

Houdusse, A., V. N. Kalabokis, D. Himmel, A. G. Szent-Gyorgyi, and C. Cohen. 1999. Atomic structure of scallop myosin subfragment S1 complexed with MgADP: a novel conformation of the myosin head. *Cell*. 97:459–470.

Huxley, H. E. 1979. Time resolved x-ray diffraction studies on muscle. *In* Cross-Bridge Mechanism in Muscle Contraction. H. Sugi and G. H. Pollack, editors. University Park Press, Baltimore. 391–394.

Huxley, H. E., and W. Brown. 1967. The low-angle x-ray diagram of vertebrate striated muscle and its behavior during contraction and rigor. *J. Mol. Biol.* 30:383–434.

Irving, M., V. Lombardi, G. Piazzesi, and M. A. Ferenczi. 1992. Myosin head movements are synchronous with the elementary force-generating process in muscle. *Nature (Lond.).* 357:156–158.

Jahn, W., C. Urbanke, and J. Wray. 1999. Fluorescence temperature jump studies of myosin S1. *J. Anat.* In press.

Johnson, K. A., and E. W. Taylor. 1978. Intermediate states of subfragment 1 and actosubfragment 1 ATPase: reevaluation of the mechanism. *Biochemistry.* 17:3432–3442.

Kensler, R., S. Peterson, and M. Norberg. 1994. The effects of changes in temperature or ionic strength on isolated rabbit and fish skeletal muscle thick filaments. *J. Muscle Res. Cell Motil.* 15: -79.

Kensler, R. W., and M. Stewart. 1993. The relaxed crossbridge pattern in isolated rabbit psoas muscle thick filaments. *J. Cell Sci.* 105:841–848.

Kensler, R. W., and J. L. Woodhead. 1995. The chicken muscle thick filament: Temperature and the relaxed cross-bridge arrangement. *J. Muscle Res. Cell Motil.* 16: -90.

Kraft, T., J. M. Chalovich, L. C. Yu, and B. Brenner. 1995. Parallel inhibition of active force and relaxed fiber stiffness by caldesmon fragments at physiological ionic strength and temperature conditions: additional evidence that weak cross-bridge binding to actin is an essential intermediate for force generation. *Biophys. J.* 68:2404–2418.

Kress, M., H. E. Huxley, A. R. Faruqi, and J. Hendrix. 1986. Structural changes during activation of frog muscle studied by time-resolved x-ray diffraction. *J. Mol. Biol.* 188:325–342.

Levine, R. J. 1993. Evidence for overlapping myosin heads on relaxed thick filaments of fish, frog, and scallop striated muscles. *J. Struct. Biol.* 110:99–110.

Levine, R. J., P. D. Chantler, and R. W. Kensler. 1988. Arrangement of myosin heads on Limulus thick filaments. *J. Cell Biol.* 107:1739–1747.

Levine, R. J., R. W. Kensler, Z. Yang, J. T. Stull, and H. L. Sweeney. 1996. Myosin light chain phosphorylation affects the structure of rabbit skeletal muscle thick filaments. *Biophys. J.* 71:898–907.

Lowy, J., D. Popp, and A. A. Stewart. 1991. X-ray studies of order-disorder transitions in the myosin heads of skinned rabbit psoas muscles. *Biophys. J.* 60:812–824.

Ma, Y. Z., and E. W. Taylor. 1994. Kinetic mechanism of myofibril ATPase. *Biophys. J.* 66:1542–1553.

Malinchik, S., S. Xu, and L. C. Yu. 1997. Temperature-induced structural changes in the myosin thick filament of skinned rabbit psoas muscle. *Biophys. J.* 73:2304–2312.

Maw, M., and A. J. Rowe. 1980. *Nature (Lond.).* 286:412–414.

Mendelson, R. A., D. K. Schneider, and D. B. Stone. 1996. Conformations of myosin subfragment 1 ATPase intermediates from neutron and X-ray scattering. *J. Mol. Biol.* 256:1–7.

Ostap, E. M., V. A. Barnett, and D. D. Thomas. 1995. Resolution of three structural states of spin-labeled myosin in contracting muscle. *Biophys. J.* 69:177–188.

Pate, E., K. Franks-Skiba, H. White, and R. Cooke. 1993. The use of differing nucleotides to investigate cross-bridge kinetics. *J. Biol. Chem.* 268:10046–10053.

Piazzesi, G., M. Reconditi, I. Dobbie, M. Linari, P. Boesecke, O. Diat, M. Irving, and V. Lombardi. 1999. Changes in conformation of myosin heads during the development of isometric contraction and rapid shortening in single frog muscle fibres. *J. Physiol. (Lond.).* 514:305–312.

Padron, R., L. Alamo, J. Murgich, and R. Craig. 1998. Towards an atomic model of the thick filaments of muscle. *J. Mol. Biol.* 275:35–41.

Rapp, G., M. Schrumpf, and J. Wray. 1991. Kinetics of the structural change in the myosin filaments of relaxed psoas fibres after a millisecond temperature-jump. *Biophys. J.* 59:35*a*. (Abstr.).

Regnier, M., and E. Homsher. 1998. The effect of ATP analogs on posthydrolytic and force development steps in skinned skeletal muscle fibers. *Biophys. J.* 74:3059–3071.

Rome, E., G. Offer, and F. A. Pepe. 1973. X-ray diffraction of muscle labelled with antibody to C-protein. *Nat. New Biol.* 244:152–154.

Schlichting, I., and J. Wray. 1986. Behaviour of crossbridges in non-overlap frog muscle in the presence and absence of ATP. *J. Muscle Res. Cell Motil.* 7:79.

Sleep, J. A., and R. L. Hutton. 1978. *Biochemistry.* 17:5423–5430.

Smith, C. A., and I. Rayment. 1996. X-ray structure of the magnesium II · ADP · vanadate complex of the *Dictyostelium discoideum* myosin motor domain to 1.9 Å resolution. *Biochemistry.* 35:5404–5417.

Squire, J. 1981. The Structural Basis of Muscular Contraction. Plenum Press, New York.

Squire, J. M. 1972. General model of myosin filament structure. II. Myosin filaments and cross-bridge interactions in vertebrate striated and insect flight muscles. *J. Mol. Biol.* 72:125–138.

Stewart, M., and R. W. Kensler. 1986. Arrangement of myosin heads in relaxed thick filaments from frog skeletal muscle. *J. Mol. Biol.* 192: 831–851.

Taylor, E. W. 1977. Transient phase of adenosine triphosphate hydrolysis by myosin, heavy meromyosin, and subfragment 1. *Biochemistry.* 16: 732–739.

Wakabayashi, K. 1992. Small-angle synchrotron x-ray scattering reveals distinct shape changes of the myosin head during hydrolysis of ATP. *Science.* 258:443–447.

Wakabayashi, T., T. Akiba, K. Hirose, A. Tomioka, M. Tokunaga, C. Suzuki, C. Toyoshima, K. Sutoh, K. Yamamoto, T. Matsumoto, K. Sacki, and Y. Amemiya. 1988. Temperature induced changes of thick filament and location of the functional site of myosin. *In* Molecular Mechanism of Muscle Contraction. H. Sugi and G. H. Pollack, editors. Plenum Publishing Co., New York. 39–48.

Walker, M., and J. Trinick. 1988. Visualization of domains in native and nucleotide-trapped myosin heads by negative staining. *J. Muscle Res. Cell Motil.* 9:359–366.

White, H. D. 1985. Kinetics of tryptophan fluorescence enhancement in myofibrils during ATP hydrolysis. *J. Biol. Chem.* 260:982–986.

White, H., B. Belknap, and M. R. Webb. 1997. Kinetics of nucleoside triphosphate cleavage and phosphate release steps by associated rabbit skeletal actomyosin, measured using a novel fluorescent probe for phosphate. *Biochemistry.* 36:11828–11836.

Wray, J. 1987. Structure of relaxed myosin filaments in relation to nucleotide state in vertebrate skeletal muscle. *J. Muscle Res. Cell Motil.* 8:62*a*. (Abstr.).

Wray, J., R. S. Goody, and K. Holmes. 1986. Towards a molecular mechanism for the crossbridge cycle. *Adv. Exp. Med. Biol.* 226:49–59.

Xie, L., W. X. Li, T. Rhodes, H. White, and M. Schoenberg. 1999. Transient kinetic analysis of N-phenylmaleimide-reacted myosin subfragment-1. *Biochemistry.* 38:5925–5931.

Xu, S., J. Gu, and L. C. Yu. 1999a. Conformational changes in cross-bridges induced by MgADP+VO_4 as a function of temperature in skinned rabbit psoas muscle fibers. *Biophys. J.* 76:164*a*. (Abstr.).

Xu, S., J. Gu, and L. C. Yu. 1999b. Characterizing and modeling the structure of weakly attached cross-bridges in the A · M·ATP state in skinned rabbit psoas muscle. *Biophys. J.* 76:33*a*. (Abstr.).

Xu, S., S. Malinchik, D. Gilroy, Th. Kraft, B. Brenner, and L. C. Yu. 1997. X-ray diffraction studies of cross-bridges weakly bound to actin in relaxed skinned fibers of rabbit psoas muscle. *Biophys. J.* 73:2292–2303.

Xu, S., and L. C. Yu. 1998. Nucleotide dependence for forming helices by myosin heads in rabbit skinned psoas muscle fibers. *Biophys. J.* 74:22*a*. (Abstr.).

Xu, S., L. C. Yu, and M. Schoenberg. 1998. Behavior of N-phenylmaleimide-reacted muscle fibers in magnesium-free rigor solution. *Biophys. J.* 74:1110–1114.